JACS
JOURNAL OF THE AMERICAN CHEMICAL SOCIETY
Article
pubs.acs.org/JACS

A Highly Selective Ratiometric Two-Photon Fluorescent Probe for Human Cytochrome P450 1A

Zi-Ru Dai,[†,§] Guang-Bo Ge,[†,‡,§] Lei Feng,[†,‡,§] Jing Ning,[†] Liang-Hai Hu,[⊥] Qiang Jin,[†] Dan-Dan Wang,[†] Xia Lv,[†] Tong-Yi Dou,[†] Jing-Nan Cui,[*,‡] and Ling Yang[*,†]

[†]Dalian Institute of Chemical Physics, Chinese Academy of Sciences, Dalian 116023, China
[‡]State Key Laboratory of Fine Chemicals, Dalian University of Technology, Dalian 116024, China
[⊥]Research Center for Drug Metabolism, College of Life Science, Jilin University, Changchun 130012, China

Supporting Information

ABSTRACT: Cytochrome P450 1A (CYP1A), one of the most important phase I drug-metabolizing enzymes in humans, plays a crucial role in the metabolic activation of procarcinogenic compounds to their ultimate carcinogens. Herein, we reported the development of a ratiometric two-photon fluorescent probe **NCMN** that allowed for selective and sensitive detection of CYP1A for the first time. The probe was designed on the basis of substrate preference of CYP1A and its high capacity for *O*-dealkylation, while 1,8-naphthalimide was selected as fluorophore because of its two-photon absorption properties. To achieve a highly selective probe for CYP1A, a series of 1,8-naphthalimide derivatives were synthesized and used to explore the potential structure−selectivity relationship, by using a panel of human CYP isoforms for selectivity screening. After screening and optimization, **NCMN** displayed the best combination of selectivity, sensitivity and ratiometric fluorescence response following CYP1A-catalyzed *O*-demetylation. Furthermore, the probe can be used to real-time monitor the enzyme activity of CYP1A in complex biological systems, and it has the potential for rapid screening of CYP1A modulators using tissue preparation as enzyme sources. **NCMN** has also been successfully used for two-photon imaging of intracellular CYP1A in living cells and tissues, and showed high ratiometric imaging resolution and deep-tissue imaging depth. In summary, a two-photon excited ratiometric fluorescent probe **NCMN** has been developed and well-characterized for sensitive and selective detection of CYP1A, which holds great promise for bioimaging of endogenous CYP1A in living cells and for further investigation on CYP1A associated biological functions in complex biological systems.

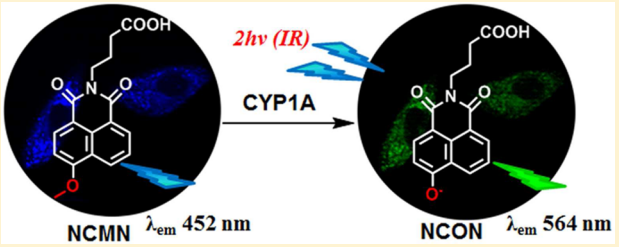

INTRODUCTION

Cytochrome P450s (CYPs) comprise a superfamily of multifunctional heme-thiolate proteins that play an important role in the oxidative metabolism of various xenobiotics and endogenous compounds.[1,2] The CYP1A subfamily has been extensively studied because of its capacity to catalyze a vast number of endogenous substrates, environmental toxins and clinical drugs.[3−5] CYP1A enzymes are mainly localized to the endoplasmic reticulum of various mammalian cells and play a key role in bioactivation of a wide range of procarcinogenic compounds (such as aflatoxins, heterocyclic aromatic amines and polycyclic aromatic hydrocarbons) to endotoxic intermediates or ultimate carcinogens, which contribute to tumor formation and thus increase the incidence of cancers.[6,7] Notably, both the expression and function of CYP1A can be modulated by a variety of therapeutic drugs and environmental factors, such as high-level aflatoxin exposure and smoking.[8] Thus, there is an imperative need to develop a practical method for rapid, sensitive detection and real-time monitoring of the enzyme activity of CYP1A in biological systems, which will be very helpful to evaluate individual variations in CYP1A-involved drug disposition and to identify the potential abnormalities of this cancer-associated enzyme.

In humans, CYP1A subfamily consists of two members, CYP1A1 and 1A2. These two isoforms share highly conserved amino acid sequence homology and overlapping substrate spectra, but differ with respect to tissue-specific expression.[9] CYP1A1 is generally expressed in extra-hepatic tissues, such as lung epithelium, skin, and placenta,[10,11] whereas CYP1A2 is abundantly expressed in liver, representing ∼4−16% of the total hepatic P450 pool.[12] In contrast to other CYPs, CYP1A exhibits relatively planar and small active cavity and shows a certain preference for dealkylation of polycyclic aromatic compounds (such as theophylline and phenacetin).[13] Another structural feature of CYP1A is that its active cavity is rich of hydroxyl amino acids, and some of which (such as Thr-118, Ser-122, Thr-124 in CYP1A2 or Ser-116, Ser-120 and Ser-122 in CYP1A1) have been reported to play key roles in substrate binding via hydrogen bond (H-bond) interactions.[14] These

Received: September 18, 2015
Published: October 21, 2015

DOI: 10.1021/jacs.5b09854
J. Am. Chem. Soc. 2015, 137, 14488−14495

findings indicate that H-bond and $\pi-\pi$ interactions may contribute to CYP1A-substrate binding and/or catalysis.

In the past decades, molecular fluorescence probes have been widely used to monitor the key enzymes in human biological processes, owing to their high selectivity, nondestructiveness, easy management, as well as capability of being applicable to high-throughput screening.[15−17] Although several fluorescent probes for CYP1A have been reported and applied to measure its activity in tissue samples,[18,19] all of these traditional fluorescent probes work with one photo microscopy (OPM) and detect CYP1A activity by intensity-responsive fluorescence signal, which can be interfered with the excitation and emission efficiency, probe concentration, and environmental conditions.[20,21] In contrast, ratiometric fluorescent probes provide the practical advantage of built-in corrections for such variability by employing the ratio of two different bands in the emission spectra.[22−25] Furthermore, two-photon excited (TPE) fluorescent probe based bioimaging can obtain improved three-dimensional spatial localization and increased imaging depth, as well as reduce phototoxicity or photodamage to biological samples over traditional single-photon excited fluorescent probes.[26−29] Therefore, it is highly desirable to combine the advantages of ratiometric fluorescent probe with two-photon microscopy (TPM) imaging for precise detection of target enzyme(s), especially in complex biological systems.

This study aimed to develop a novel ratiometric two-photon fluorescent probe for highly selective sensing the enzyme activity of CYP1A in complex biological systems. 4-Hydroxy-1,8-naphthalimide (**HN**) was selected as the basic fluorophore as it possesses a polycyclic aromatic skeleton and has desirable photophysical properties, such as large Stokes shifts, high photostability and significant two-photon absorbability at near-infrared wavelength.[30−33] Modulation of the electron donating ability of C-4 phenol group will trigger significant changes in both absorption and emission spectra, which makes **HN** and its derivatives desirable ratiometric two-photon fluorescence probes based on the mechanism of internal charge transfer (ICT).[34] In our preliminary study, a series of *O*-alkylated **HN** derivatives were synthesized to evaluate their potential as good substrates of CYP1A (Table S1). The initial screening revealed that 4-methoxy-1,8-naphthalimide (**MN**) displayed ideal reactivity toward CYP1A. Nevertheless, it can also be rapidly *O*-demethylated by other CYPs including CYP2B6 and CYP2C19 (Table S1). To improve their selectivity toward CYP1A, a series of N-substituted **MN** derivatives were synthesized. Given that the active cavity of CYP1A was rich of hydroxyl amino acids, several N-substitutes with hydrogen bond acceptor were purposely introduced into the **HN** skeleton. Among these newly synthesized N-substituted **HN** derivatives, *N*-(3-carboxy propyl)-4-methoxy-1,8-naphthalimide (**NCMN**) displayed good reactivity and high selectivity toward CYP1A over other CYPs isoforms. The methoxy group of **NCMN** could be selectively cleaved by CYP1A, leading to the release of *N*-(3-carboxy propyl)-4-hydroxy-1,8-naphthalimide (**NCHN**). As a result, CYP1A-mediated **NCMN**-*O*-demethylation led to discernible color changes and substantial red-shifted fluorescence emission (Scheme 1). These findings promoted us to further characterize the selectivity and sensitivity of this CYP1A probe, and explore the feasibility and practicability of its use in complex biological systems.

Scheme 1. Structure of NCMN and Its Fluorescence Response toward CYP1A

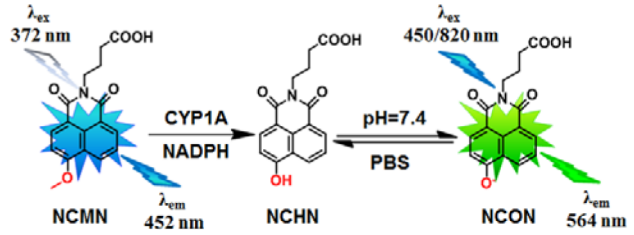

RESULTS AND DISCUSSION

Design and Synthesis of NCMN. **NCMN** could be readily synthesized with *N*-(3-carboxy propyl)-4-bromo-1,8-naphthalimide as the starting materials (Scheme S1) and its structure was fully characterized by ^{1}H NMR, ^{13}C NMR and HRMS spectra (Supporting Information). **NCMN** could be metabolized to form a single metabolite upon the addition of human liver microsome (HLM), or CYP1A in the NADPH-generating system under physiological conditions (pH 7.4 at 37 °C). The formation of this metabolite was time-, NADPH-, and enzyme-dependent. The metabolite was identified as **NCHN** by comparison of LC retention times, UV and MS spectra with the help of standard (Figure S2). As shown in Figure 1a and 1b,

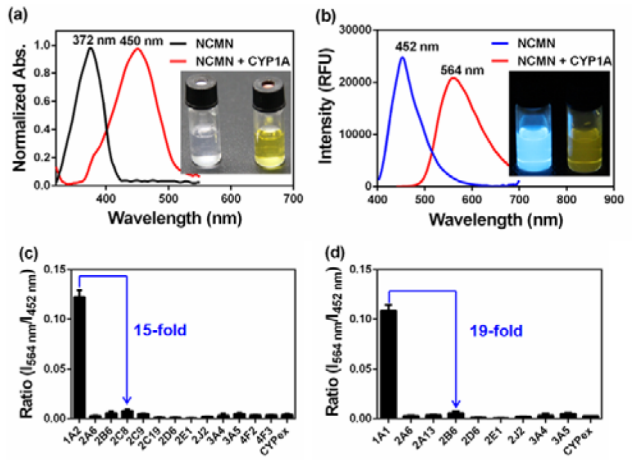

Figure 1. (a) Normalized absorption spectra of **NCMN** (20 μM) upon addition of CYP1A (100 nM). (b) Emission spectra of **NCMN** (20 μM) upon addition of CYP1A (100 nM). Fluorescence responses of **NCMN** (100 μM) toward various species of enzymes in HLM (c) and HLuM (d).

NCMN-*O*-demethylation brought a remarkable fluorescence enhancement at 564 nm (for metabolite), accompanying with a gradually decrease in the emission peak at 452 nm (for **NCMN**). Meanwhile, the color of the incubated samples turned from colorless to yellow, indicating that **NCMN** could serve as a "'naked-eye'" colorimetric indicator for target enzyme(s). More importantly, the large emission shift with a desirable red-shifted emission after biotransformation (112 nm) implied that this probe could serve as a ratiometric florescence probe to measure the catalytic activity of target enzyme(s) in human biological samples. Of note, to test the feasibility of **NCMN** as a CYP1A probe, the performance of **NCMN** and **NCHN** in phosphate buffer saline (PBS) with different pH values ranging from 2 to 10 was tested. As shown in Figure S3, pH of the medium displayed negligible effects on the fluorescence

DOI: 10.1021/jacs.5b09854
J. Am. Chem. Soc. 2015, 137, 14488−14495

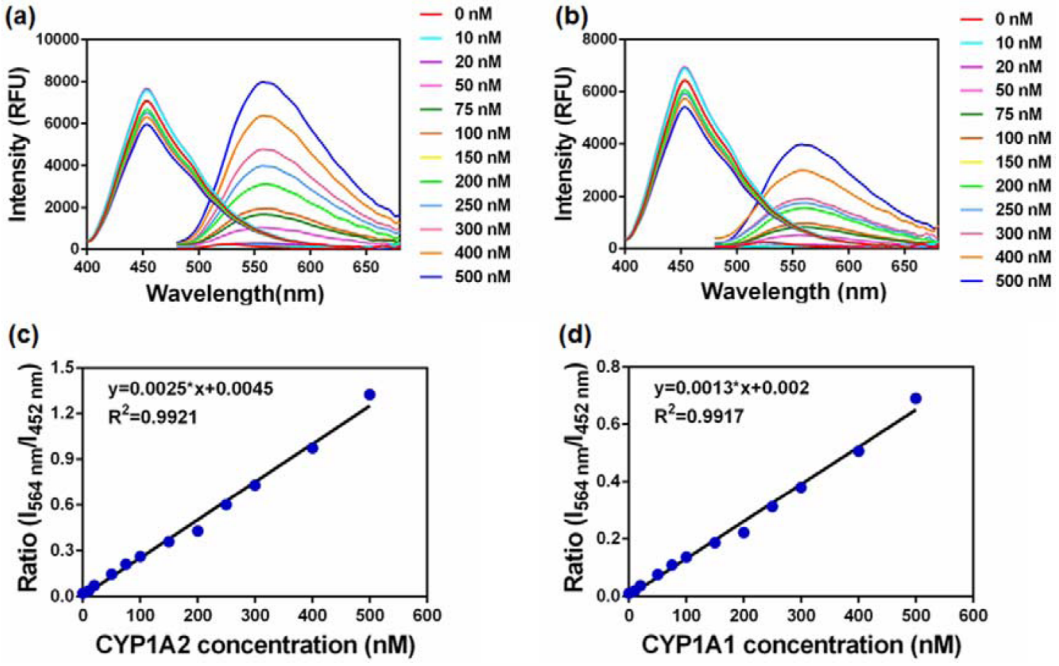

Figure 2. Fluorescence spectra changes of **NCMN** (10 μM) in the presence of increasing CYP1A2 (a) and CYP1A1 (b) in reaction system incubated for 50 min. Concentration-dependent fluorescence intensity ratios change at 452 and 564 nm (I_{564} nm/I_{452} nm) of **NCHN** to **NCMN** (10 μM) in the presence of increasing CYP1A2 (c) and CYP1A1 (d) after incubation for 50 min.

intensity for both **NCMN** and **NCHN** over the pH range of 7.0−10.0, suggesting that **NCMN** could function properly under physiological conditions (pH 7.4).

Selectivity Screening of NCMN. The selectivity of **NCMN** was investigated by a series of P450 isoforms distributed in human liver and lung.[35,36] As shown in Figure 1c and Figure 1d, CYP1A1 and CYP1A2 caused remarkable changes in fluorescence spectrum, whereas no obvious changes in fluorescence were observed upon addition of other CYP isoforms. The **NCMN** demethylation rates in both CYP1A1 and CYP1A2 are 15-fold higher than that in other human CYPs. These results suggested that **NCMN** was highly selective for CYP1A over other human CYPs. To further validate the selectivity of **NCMN** in complex biological systems (such as human liver preparations), chemical inhibition assays were conducted in HLM by using selective inhibitors of major human CYP isoforms. As shown in Figure S4, the formation of **NCHN** could be potently inhibited by ABT (a broad CYP inhibitor) and furafylline (a selective and potent inhibitor of CYP1A).[37] In contrast, inhibitors of other CYP isoforms displayed minor effects on this (CYP1A mediated) biotransformation. These results indicated that the **NCMN**-*O*-demethylation was selectively catalyzed by CYP1A in human tissues.

Fluorescence Sensing Behavior of NCMN toward CYP1A. Next, the linear response ranges for CYP1A quantification with **NCMN** as probe substrate were evaluated under physiological conditions. As shown in Figure S5, the formation rates of **NCHN** in both CYP1A1 and CYP1A2 were linear with reaction time, the ratio of fluorescence intensities (564 nm/452 nm) exhibited a good linearity (R^2 > 0.99) with the incubation time up to 50 min. On the basis of these findings, the following assays related to quantitative analysis for CYP1A were conducted within 50 min. The detection limits of **NCMN** for CYP1A were evaluated as 0.02 nmol·mL^{-1} and 0.05 nmol·mL^{-1}, in CYP1A2 and CYP1A1, respectively (Figure S6).

The responses of **NCMN** toward target enzymes with different concentrations were also investigated. As shown in Figure 2, good linearity relationships (R^2 > 0.99) between the fluorescence intensity ratio (564 nm/452 nm) and enzyme concentrations in the range of 0 to 500 nM were obtained. The excellent selectivity and high reactivity of the fluorescence-based assay indicated that **NCMN** could serve as an efficient tool to measure the enzyme activities of CYP1A in biological samples.

The kinetic behavior was also crucial for the quantitative applications of the activity-based fluorescent probes.[38] In this study, the kinetic behaviors of **NCMN**-*O*-demethylation were well characterized in different enzyme sources including recombinant CYP1A2, CYP1A1, HLM and HLuM (human lung microsomes). **NCMN**-*O*-demethylation in these enzyme sources followed the classic Michaelis−Menten kinetics, as evidenced by the corresponding Eadie-Hofstee plots (Figure S7). As shown in Table 1, **NCMN**-*O*-demethylation in both HLM and CYP1A displayed high affinity (K_m < 12 μM) and good reactivity (k_{cat}/K_m > 1.0 nmol·min^{-1}·nmol^{-1} CYP). In contrast to HLM, HLuM displayed much lower reactivity for **NCMN**-*O*-demethylation, which could be attributed to the low

Table 1. Kinetic Parameters of NCMN-*O*-Demethylation Determined in Different Enzyme Sources[a]

enzyme sources	k_{cat}	K_m (μM)	k_{cat}/K_m
HLM (pooled)	25.61 ± 0.15	9.54 ± 0.24	2684.48
CYP1A2	32.06 ± 0.50	9.80 ± 0.67	3271.43
HLuM (pooled)	2.76 ± 0.03	7.92 ± 0.44	348.48
CYP1A1	17.44 ± 0.20	11.99 ± 0.53	1454.54

[a] k_{cat} values were in nmol min^{-1} mg^{-1} protein for liver and lung microsomes, or in nmol min^{-1} nmol^{-1} CYP for CYP1A. The range of substrate concentrations was 1 to 150 μM. Each value was the mean ± SD of determinations performed in duplicate.

DOI: 10.1021/jacs.5b09854
J. Am. Chem. Soc. 2015, 137, 14488−14495

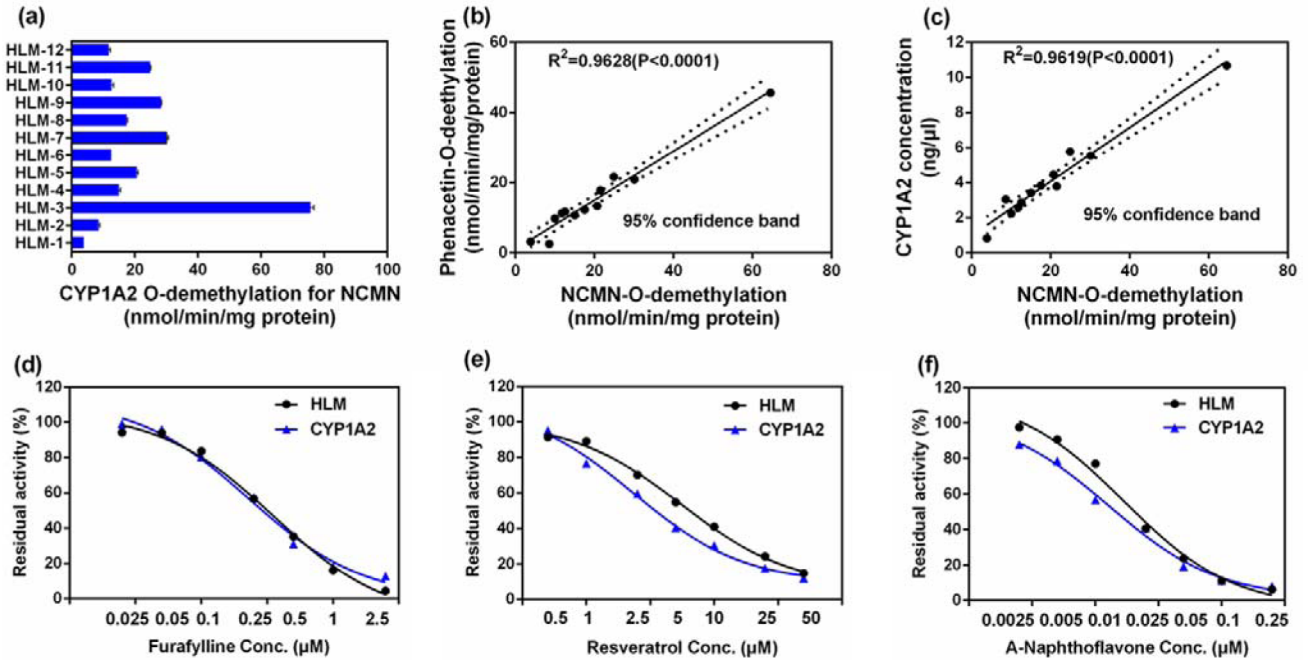

Figure 3. (a) The catalytic activities of CYP1A in 12 individual HLMs using **NCMN** as the probe substrate. (b) Correlation analysis between **NCMN** (10 μM) *O*-demethylation and phenacetin (10 μM) *O*-deethylation. (c) Correlation analysis between **NCMN** (10 μM) *O*-demethylation and the level of CYP1A2 by HLMs from individuals. The activities for **NCMN** were expressed by the formation rate of **NCHN** ($\lambda_{ex}/\lambda_{em}$ = 450/564 nm). Dose-inhibition curves of furafylline (0.025−2.5 μM) (d), resveratrol (0.5−50 μM) (e), and α-naphthoflavone (0.0025−0.25 μM) (f) on **NCMN** (20 μM) *O*-demethylation in HLM (0.25 mg/mL) and CYP1A2 (100 nM).

expression of CYP1A1 in human lung.[39] To the best of our knowledge, this is the first time to characterize the enzyme kinetics of CYP1A in human extrahepatic tissue preparations. These results demonstrated that **NCMN**-*O*-demetylation exhibited good reactivity and ideal kinetic behaviors, which prompted us to apply this probe for quantitative measurement of CYP1A in complex biological samples.

Quantification of CYP1A in Human Liver Microsomes. As shown in Figure 3a, the catalytic activities of CYP1A mediated **NCMN**-*O*-demethylation in a panel of 12 HLMs from different individuals were depicted. More than 15-fold variations in the catalytic activity were observed, in good agreement with the previously reported results in CYP1A activity obtained from individual HLMs.[40] These data were then compared with the corresponding catalytic activities of CYP1A in these individual samples, as determined by a traditional nonflorescent probe (phenacetin) of CYP1A. As shown in Figure 3b, the *O*-demethylation rates of **NCMN** were highly consistent with the *O*-deethylation rates of phenacetin in these individual HLMs. Furthermore, the rates of **NCMN**-*O*-demethylation also agreed well with the levels of CYP1A2 in these individual HLMs, which were determined by a proteomics-based approach (Figure 3c).[41] These results confirmed that **NCMN**-*O*-dealkylation exhibited excellent selectivity toward CYP1A in human liver.

High-Throughput Screening of CYP1A Inhibitors. Encouraged by the above-mentioned findings, we subsequently employed **NCMN** as a fluorescent substrate to rapidly screen CYP1A inhibitors. Three known inhibitors of CYP1A including furafylline, resveratrol and a-naphthoflavone were used, and their inhibitory effects on CYP1A mediated **NCMN**-*O*-dealkylation in both HLM and recombinant human CYP1A2 were evaluated. As expected, the inhibitory tendency and IC_{50} values of these three inhibitors were consistent in these different enzyme sources, indicating that HLM could be used as the enzyme source instead of the more expensive recombinant CYP1A in such assays (Figure 3d, 3e and 3f). These findings demonstrated that **NCMN** could serve as a highly selective florescence probe for high-throughput screening and characterization of CYP1A modulators using human liver preparations as enzyme sources.

Two-Photon Properties of NCMN. The two-photon absorption cross sections of **NCMN** and **NCHN** were determined by the two-photon induced fluorescence measurement technique. As shown in Figure S8, both **NCMN** and **NCHM** could be excited with near-infrared light (two-photon absorption), while the two-photon action cross section ($\Phi\delta$) values of both substrate and product were much close under excitation at 820 nm (74 and 72 GM, respectively). These results suggested that this probe could serve as a two-photon ratiometric fluorescent probe for imaging of CYP1A in living specimens with considerable high resolution and sensitivity.

Bioimaging Applications in Living Cells. To further expand the potential applications of this newly developed probe in bioimaging related fields, especially cellular fluorescence imaging, **NCMN** was intentionally applied for bioimaging of endogenous CYP1A in living A549 and HepG2 cells. A methyl ester derivative of **NCMN** (**NCMNe**) with improved permeability was synthesized and characterized (Figure S9),[42,43] which could be rapidly hydrolyzed by human esterases to release **NCMN**. The cell viability of A549 and HepG2 cells in the presence of both **NCMN** and **NCMNe** were examined by a standard MTT assay. As shown in Figure S10, both **NCMN** and **NCMNe** exhibited relatively low toxicity toward the human cells examined. Particularly, no obvious cytotoxicity was observed in the presence of **NCMNe** even at high concentration (100 μM) at 37 °C for 48 h. **NCMNe** was then

DOI: 10.1021/jacs.5b09854
J. Am. Chem. Soc. 2015, 137, 14488−14495

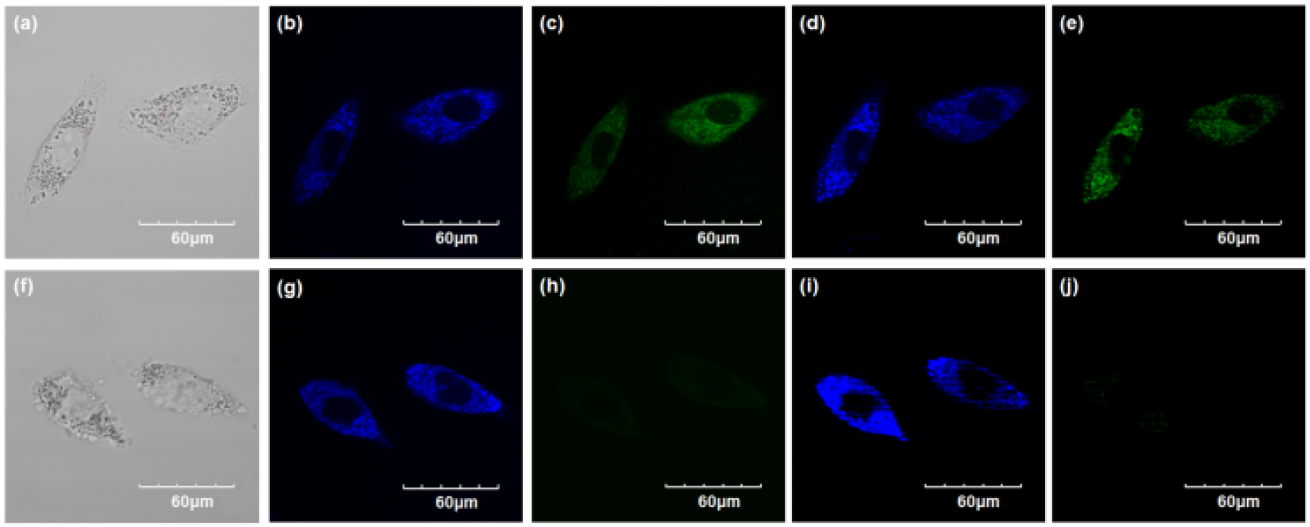

Figure 4. Confocal fluorescence images of A549 cells. Cells incubated with **NCMNe** (50 μM) for 1h (top); cells pretreated with Furafylline (50 μM) and then incubated with **NCMNe** for 1 h (bottom). Single photon images were acquired using 405 nm excitation and fluorescent emission windows: (a,f) bright-field images; (b,g) blue emission channel; (c,h) green emission channel. Two photon images were acquired using 820 nm excitation and fluorescence emission windows: (d,i) blue = 420−460 nm; (e,j) green = 495−540 nm. Scale bar: 60 μm.

used for imaging endogenous CYP1A in living A549 and HepG2 cells.

A549 cells were loaded with **NCMNe** (50 μM) at 37 °C for 1 h and subsequently washed with PBS buffer to remove the free probes, which ensured probes to be mainly localized in the targeted organelles. As expected, the cells exhibited both single-photon and two-photon excited intense intracellular fluorescence in blue and green channel (Figure 4a−e), corresponding to the fluorescence of substrate at 452 nm and the fluorescence of product at 564 nm. In sharp contrast, upon pretreatment of cells with CYP1A selective inhibitor furafylline (50 μM), the fluorescence intensity decreased significantly in the green channel and increased evidently in the blue channel (Figure 4f−j). It was evident that the changes in fluorescence response were dependent on the intracellular CYP1A-mediated **NCMN**-*O*-demethylation. Hence, these data showed that **NCMN** could be used for both single-photon and two-photon-excited bioimaging and for sensing the real activity of CYP1A in living cells.

NCMNe could also be applied for quantitative detection of CYP1A in both intact cells and cell homogenate. To demonstrate this potential use, a known CYP1A inducer (2,3,7,8-tetrachlorodibenzo-p-dioxin, TCDD) was used to evaluate its effects on the expression and activity of CYP1A in HepG2 cells.[44] As shown in Figure 5 and Figure 6, two different concentrations of TCDD (1 and 10 nM) were used to stimulate the expression of CYP1A in living HepG2 cells. After coincubation with TCDD for 3 days, HepG2 cells showed strong fluorescence responses in green channel (Figure 5d−f), corresponding to the fluorescence of **NCHN** at 564 nm. In contrast to the control samples (without TCDD), there was an 11-fold increase in CYP1A activity in cell homogenate upon addition of 10 nM TCDD (Figure 6a). Furthermore, the elevated CYP1A activities were consistent with the increased protein levels of CYP1A as assayed by Western blot analysis (Figure 6b and Figure S11). These findings clearly showed that **NCMN** could be used to screen potent CYP1A inducers and to determine the enzyme activity of endogenous CYP1A in living cells.

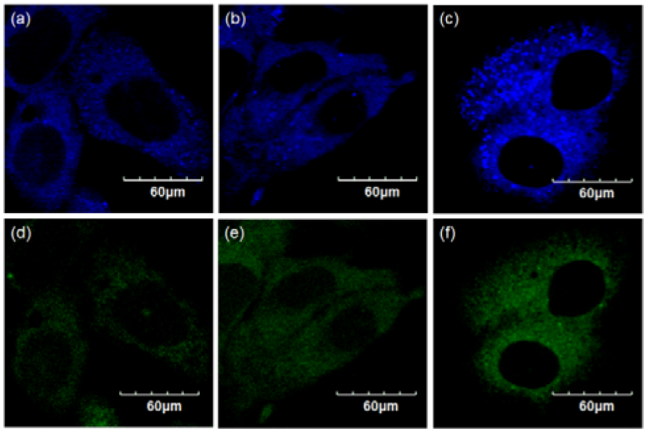

Figure 5. Two-photon confocal fluorescence images of HepG2 cells. Cells incubated with **NCMNe** (50 μM) for 1 h (a,d); cells pretreated with TCDD (1 nM) (b,e) ; TCDD (10 nM) (c,f) and then incubated with **NCMNe** for 1 h. Images were acquired using 820 nm excitation and fluorescence emission windows: blue = 420−460 nm (a−c), green = 495−540 nm (d−f). Scale bar: 60 μm.

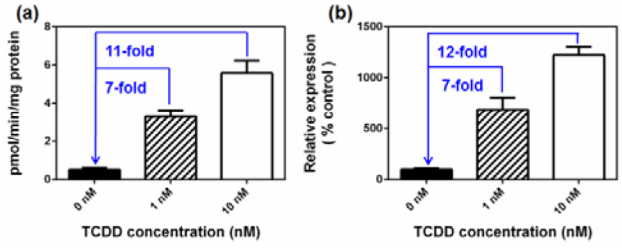

Figure 6. (a) **NCMN** *O*-demethylation by cell homogenates prepared from HepG2 cells pretreated with TCDD (0,1,10 nM). (b) The levels of CYP1A in HepG2 cells were analyzed by Western blots. Data are shown as mean ± SD (n = 3).

3D Depth Imaging of CYP1A in Rat Liver Tissues. To further assess the performance of **NCMN** for bioimaging applications, we investigated the applicability of this probe for tissue imaging. Prior to tissue imaging, the specificity of **NCMN**

DOI: 10.1021/jacs.5b09854
J. Am. Chem. Soc. 2015, 137, 14488−14495

toward CYP1A in rat liver was investigated first. As shown in Figure S12, **NCMN** could be rapidly dealkylated in rat liver preparations, while **NCMN**-*O*-demethylation could be significantly blocked by several known selective inhibitors of CYP1A, suggesting that **NCMN**-*O*-demethylation in rat liver is also CYP1A dependent. Next, a slice of liver freshly isolated from a 7-week-old rat was incubated with 50 μM **NCMNe** for 1h at 37 °C. As shown in Figure 7a and 7b, these TPM images revealed

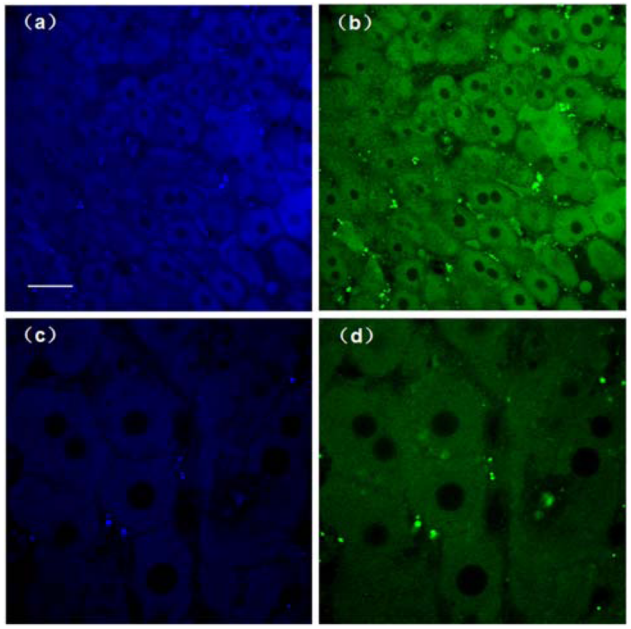

Figure 7. TPM images of a fresh rat liver slice stained with 50 μm **NCMNe** at depth of ≈100 μm with magnification at 60× (a,b) and 100 × (c,d). Images were acquired using 820 nm excitation and fluorescent emission windows: (a,c) blue = 420−460 nm; (b,d) green = 495−540 nm. Scale bars: 30 μm.

strong fluorescence responses in both blue and green channels at a depth of 100 μm, indicating that CYP1A are abundant in rat liver. Consistently, CYP1A was also found abundantly expressed in individual cells (Figure 7c and 7d). Moreover, the TPM images at the depths 20, 40, 60, 80, 100, and 120 μm showed the CYP1A distribution in each xy plane along the z direction (Figure S13). All these results demonstrated that **NCMN** displayed good capability of tissue penetration and was suitable for direct two-photon fluorescent depth imaging of ultratrace CYP1A in tissues.

Docking Simulation of NCMN into the Reported Structure of CYP1A2 and CYP1A1. Molecular modeling study was carried out to provide deep insight into CYP1A-mediated **NCMN** *O*-demethylation. As shown in Figure 8, **NCMN** could be well docked into the active cavity of CYP1A2 and CYP1A1. Three similar H-bonds between **NCMN** and CYP1A2 (with Thr-118, Thr-124, and Asp-313), and CYP1A1 (with Ser-116, Ser-122, and Asp-313) were observed. Notably, the carboxyl group of **NCMN** could form an H-bond with Thr-124 in CYP1A2 or Ser-122 in CYP1A1, implying that the carboxyl group played an important role in the recognition and binding of CYP1A through H-bond interactions, as expected in the probe design.[45] As a result, the hammerhead score value of the bioactive pose of **NCMN** in CYP1A2 (−34.83) is slightly higher than that in CYP1A1 (−30.36), which is consistent with the binding affinity values of **NCMN** toward these two isoforms

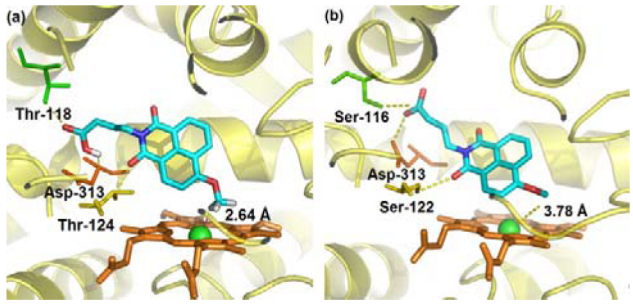

Figure 8. Docking simulation of **NCMN** into CYP1A2 (a) and CYP1A1 (b). Heme and iron atoms are colored with brown and green, respectively.

(Table S2). In addition, molecular docking studies showed that **NCMN** could orient itself better in the active site of CYP1A2 than CYP1A1 with proton-iron distances of 2.64 and 3.78 Å, respectively. These findings may, or at least in part, account for the reason why the catalytic rate of **NCMN** by CYP1A2 is higher than that by CYP1A1 and verify the key roles of H-bond interactions in CYP1A mediated **NCMN**-*O*-demethylation.

■ CONCLUDING REMARKS

In summary, we reported the development of a highly selective ICT-based two-photon ratiometric fluorescent probe **NCMN** for ratiometric detection of human cytochrome P450 1A for the first time. The fluorescent probe **NCMN** was designed for the selective detection of CYP1A based on its catalytic function and substrate preference, as well as two-photon absorption properties of naphthalimide fluorophore. **NCMN** is a naked-eye visible and ratiometric fluorescence probe, which can be selectively dealkylated by CYP1A and trigger remarkable changes in absorption and fluorescence spectra. Because of its excellent selectivity toward CYP1A and its good fluorescence properties, **NCMN** can be used to quantify CYP1A enzyme activity and to real-time monitor the changes in CYP1A associated biological functions in complex biological systems. Meanwhile, ratiometric TPM bioimaging of **NCMN** and its metabolite revealed that this probe could also be used for real-time measurement of the enzyme activity of endogenous CYP1A in several cell lines as well as in rat liver tissues. All these features suggested that **NCMN** could serve as a promising tool for exploring the biological functions of CYP1A in xenobiotics metabolism, toxicological assessments and other related fields. Furthermore, the strategies employed in the design and optimization of this probe may shed new lights on the development of other highly specific fluorescent probes for a given drug-metabolizing enzyme.

■ EXPERIMENTAL SECTION

Full details regarding materials, synthesis and characterization of compounds, more detailed experimental procedures are described in the Supporting Information.

CYP Reaction Phenotyping Assays. Thirteen cDNA-expressed human CYP isoforms coexpressing NADPH-P450 reductase (CYP1A2, CYP2A6, CYP2B6, CYP2C8, CYP2C9, CYP2C19, CYP2D6, CYP2E1, CYP2J2, CYP3A4, CYP3A5, CYP4F2 and CYP4F3) were used to screen the involved isoform(s) for demethylation of **NCMN** in HLM, while eight cDNA-expressed human CYP isoforms (CYP1A1, CYP2A13, CYP2B6, CYP2D6, CYP2E1, CYP2J2, CYP3A4 and CYP3A5) were used to screen the involved isoform(s) in HLuM. The incubations were carried out under the above-mentioned incubation conditions with each of CYP isoform.

DOI: 10.1021/jacs.5b09854
J. Am. Chem. Soc. 2015, 137, 14488−14495

To generate adequate metabolites for detection, a relative high substrate concentration (100 μM) was used and incubated with each of the recombinant CYPs (40−80 nM) at 37 °C for 30 min.

Chemical Inhibition Assays. *O*-demethylation of **NCMN** in pooled HLM in the absence or presences of selective inhibitors for different CYP isoforms were measured to verify the involved enzyme(s) for this biotransformation. In brief, **NCMN** (10 μM, relevant to the K_m values) was incubated in HLM (0.25 mg/mL) with an NADPH-generating system in the absence (control) or presence of known CYP isoform-specific inhibitors. The selective inhibitors and their concentrations were as follows:[46] montelukast (2 μM) for CYP2C8, sulfaphenazole (10 μM) for CYP2C9, omeprazole (20 μM) for CYP2C19, quinidine (10 μM) for CYP2D6 and clomethiazole (50 μM) for CYP2E1. Inhibition by furafylline (10 μM) for CYP1A2, tranyleypromine (1 μM) for CYP2A6,[47] TEPA (50 μM) for CYP2B6, troleandomycin (200 μM) for CYP3A and ABT (500 μM) for broad CYPs were assayed by preincubation with NADPH-generating system at 37 °C for 20 min. Other procedures including termination step and sample preparation were depicted as described previously. The inhibitory effects were expressed as percent decrease in fluorescence intensities ratio (I_{564}/I_{452}). Data were fit to log (inhibitor) vs normalized response—Variable slope equation using GraphPad Prism 6 (GraphPad Software, San Diego, CA).

Enzyme Kinetics Analysis. To estimate the kinetic parameters of **NCMN** *O*-demethylation in different enzyme sources, the incubation conditions were optimized to ensure the formation rates of **NCHN** were in the linear range in relation to incubation time and protein concentration at 37 °C. **NCMN** (dissolved in acetonitrile previously) was serially diluted to the required concentrations (2.5, 5, 10, 25, 50, 75, 100, 150 μM), and the final concentration of acetonitrile was 1% (v/v). **NCMN** was incubated with pooled human liver microsomes and pooled human lung microsomes (0.25 mg protein/mL) for 25 min, or with recombinant CYP1A2 and CYP1A1 (75 nM) for 30 min. All incubations were performed in duplicate, and the fluorescence intensity was recorded continuously as described above. The relationship between [S] and [V] was plotted, and fitted to the Michaelis−Menten equation. Data analysis was performed by a nonlinear regression using GraphPad Prism 6 (GraphPad Software, San Diego, CA).

Correlation Studies. In order to evaluate the applicability of **NCMN** as a selective indicator for measurement of CYP1A activity in human biological samples, the formation rates of the metabolite(s) described for **NCMN** in a panel of 12 HLMs from individuals were determined and compared with the catalytic activities of CYP1A to their marker substrates as well as levels of CYP1A. Phenacetin was used as a probe substrate for CYP1A.[48] The demethylation of **NCMN** (10 μM near K_m values) was performed in HLM (0.25 mg/mL) for 30 min. Phenacetin (40 μM) was incubated with HLM (0.25 mg/mL) for 30 min. Phenacetin and its deethylation product were determined by LC-UV at 250 nm.[49] Then the rates of **NCMN** demethylation in 12 individual HLMs were compared with the rates of phenacetin deethylation. In addition, the formation rates of **NCMN** were also compared with the levels of CYP1A2 in 12 individual HLMs. The concentrations of CYP1A2 in HLM were determined by liquid chromatography-tandem mass spectrometer (LC-MS/MS), using multiple reaction monitoring (MRM) mode and isotope labeled peptide as the internal standards. Specific peptides of YLPNPALQR (for CYP1A2) were selected for their quantification by using transition ion of 536.3/584.3.[41] The correlation parameter was expressed by the linear regression coefficient (R^2). $P < 0.005$ was considered statistically significant.

CYP1A Inhibitors Screening. The assay was performed in a 96-well microplate. A mixture of **NCMN** (10 μM), NADPH-generating system, three CYP1A selective inhibitors of furafylline (0−2.5 μM),[50] resveratrol (0−50 μM),[51] and a-naphthoflavone (0−0.25 μM) and recombinant CYP1A2 (75 nM) or HLM (0.25 mg/mL) in potassium phosphate buffer (100 mM, pH 7.4) containing less than 1% DMSO (total volume 200 μL), was incubated for 50 min at 37 °C.[52] Fluorescence measurements were performed using a Synergy H1 Hybrid Multi-Mode Microplate Reader (Bio Tek). Inhibition percentage was calculated by comparing to control sample samples that were incubated under identical conditions, except in the absence of the inhibitors.

Cell Culture and Fluorescence Imaging. A549 (human lung cancer line) and HepG2 (human hepatoma cell line) were grown in Dulbecco's modification of Eagle's medium Dulbecco (DMEM/high: with 4.5 g/L Glucose, 4.0 mM L-Glutamine, and 110 mg/L Sodium Pyruvate), supplemented with fetal bovine serum of 10%. Washed twice with FBS-free DMEM, the adherent cells were incubated with/without 50 μM furafylline (preparing in FBS-free DMEM) for 1 h at 37 °C in CO_2 incubator of 5%. At a 50 μM final concentration, stock solution of probe **NCMNe** (5 mM) in DMSO was diluted into the cell culture media (FBS free). The cells were then incubated at 37 °C for another 1h, and then washed with PBS (pH 7.4) for three times, and then imaged on confocal microscope (Olympus, FV1000, Japan).

Tissue Slices Preparation and Two-Photon Fluorescence Imaging. Slices were prepared from the liver of 7-weeks-old rat. Slices were cut to 300 mm thickness by a vibrating-blade microtome in 25 mM PBS (pH 7.4). For the control experiments, slices were incubated with 20 mM **NCMNe** in PBS buffer bubbled with 95% O_2 and 5% CO_2 at 37 °C for 40 min. Slices were then washed three times with PBS, transferred to glass-bottomed dishes (Nest, 35 mm dish with 20 mm well), and observed under a two-photon confocal microscope (Olympus, FV1000, Japan). The two-photon fluorescence emission was collected at wavelength between 460 and 540 nm upon excitation at 820 nm with a femtosecond pulse.

Preparation of S9 Fractions and Western Blot Analysis. HepG2 cells were washed, resuspended, and sonicated in ice-cold PBS buffer. The S9 fractions were prepared following centrifugation at 9000*g* for 20 min. Supernatants were collected and protein contents were assessed by the BCA reagent assay (Beyotime, Jiangsu, CHN). Eighty mircograms of protein per sample was loaded per well on 10% polyacrylamide gels. After electrophoresis performed, the separated proteins were transferred onto Sequi-Blot PVDF membranes (Bio-Rad, Hercules, CA) in transfer buffer [192 mM glycine, 25 mM Tris-base, pH 8.3, 20% (v/v) methanol]. Membranes were blocked with 5% nonfat dried milk in TBS-T buffer [20 mM Tris-HCl, pH 8.0, 50 mM NaCl, 0.1% (v/v) Tween-20] at room temperature for 1 h. Membranes were then incubated with anti-Cytochrome P450 1A2 antibody (Abcam, Cambridge, UK) overnight at 4 °C and further incubated with HRP-conjugated anti-antibody (Abcam, Cambridge, UK) for 1 h. GAPDH (GenScript, New Jersey, USA) was used to establish as the internal standard. The blots were washed three times with TBS-T buffer, and the immunereactive protein bands were detected by enhanced chemiluminescence (Vilber Lourmat, Marne-la-Vallée, FRA).

Molecular Docking. Docking simulation was performed by using SYBYL (X-1.1). Here, the X-ray crystallographic structure of human cytochrome P450 1A2 (coded as 2HI4) and P450 1A1 (coded as 4I8 V) were selected for docking analysis. After the backbone and variable modeling, a 1000-step minimization was carried out to obtain a low-energy conformation without any steric clashes between side chains. With the crystal structure of 1A2 and 1A1, the bioactive binding conformations of **NCMN** were generated using Surflex-Dock, which were evaluated by an empirical function ChemScore, one of the most suitable scoring functions for P450s superfamily.[53]

■ ASSOCIATED CONTENT

Ⓢ Supporting Information

The Supporting Information is available free of charge on the ACS Publications website at DOI: 10.1021/jacs.5b09854.

Synthesis, characterization, experimental details and image data. (PDF)

■ AUTHOR INFORMATION

Corresponding Authors

*yling@dicp.ac.cn

*jncui@dlut.edu.cn

DOI: 10.1021/jacs.5b09854
J. Am. Chem. Soc. 2015, 137, 14488−14495

Author Contributions

[§]Z.-R.D., G.-B.G., and L.F. contributed equally.

Notes

The authors declare no competing financial interest.

■ ACKNOWLEDGMENTS

We gratefully acknowledge Prof. Zhihong Liu of Wuhan University for measurements of two-photon excitation spectra of the probe and its product, Prof. Liping Yang of Nantong Tumor Hospital for experimental guidance for the fluorescence imaging and Dr. Hailing Cheng of Harvard University and Jiayue Wang of Dalian Institute of Chemical Physics for language proofreading. This work was supported by the National S&T Major Projects of China (2012ZX09501001, 2012ZX09506001), the National Basic Research Program of China (2013CB531800), NSF of China (81573501, 81473181, 81273590), and the State Key Laboratory of Fine Chemicals (KF1304).

■ REFERENCES

(1) Coon, M. J. *Biochem. Biophys. Res. Commun.* **2005**, *338*, 378.
(2) Hasler, J. A. *Mol. Aspects Med.* **1999**, *20*, 12.
(3) Wrighton, S. A.; Stevens, J. C. *Crit. Rev. Toxicol.* **1992**, *22*, 1.
(4) Sachse, C.; Brochmoller, J.; Bauer, S.; Roots, I. *Br. J. Clin. Pharmacol.* **1999**, *47*, 445.
(5) Shimada, T.; Fujii-Kuriyama, Y. *Cancer Sci.* **2004**, *95*, 1.
(6) Boffetta, P.; Jourenkova, N.; Gustavsson, P. *Cancer Causes Control* **1997**, *8*, 444.
(7) Turner, I. M.; R, T. C. *Trends Ecol. Evol.* **1996**, *11*, 330.
(8) Zhou, S. F.; Yang, L. P.; Zhou, Z. W.; Liu, Y. H.; Chan, E. *AAPS J.* **2009**, *11*, 481.
(9) Hammons, G. J.; Milton, D.; Stepps, K.; Guengerich, F. P.; Tukey, R. H.; Kadlubar, F. F. *Carcinogenesis* **1997**, *18*, 851.
(10) Shimada, T.; Yun, C. H.; Yamazaki, H.; Gautier, J. C.; Beaune, P. H.; Guengerich, F. P. *Mol. Pharmacol.* **1992**, *41*, 856.
(11) Yengi, L. G.; Xiang, Q.; Pan, J.; Scatina, J.; Kao, J.; Ball, S. E.; Fruncillo, R.; Ferron, G.; Roland Wolf, C. *Anal. Biochem.* **2003**, *316*, 103.
(12) Agundez, J. A. *Curr. Drug Metab.* **2004**, *5*, 211.
(13) Sansen, S.; Yano, J. K.; Reynald, R. L.; Schoch, G. A.; Griffin, K. J.; Stout, C. D.; Johnson, E. F. *J. Biol. Chem.* **2007**, *282*, 14348.
(14) Dong, D.; Wu, B.; Chow, D.; Hu, M. *Drug Metab. Rev.* **2012**, *44*, 192.
(15) Zhang, H.; Fan, J.; Wang, J.; Dou, B.; Zhou, F.; Cao, J.; Qu, J.; Cao, Z.; Zhao, W.; Peng, X. *J. Am. Chem. Soc.* **2013**, *135*, 17469.
(16) Cui, L.; Zhong, Y.; Zhu, W.; Xu, Y.; Qian, X. *Chem. Commun. (Cambridge, U. K.)* **2010**, *46*, 7121.
(17) Guliyev, R.; Coskun, A.; Akkaya, E. U. *J. Am. Chem. Soc.* **2009**, *131*, 9007.
(18) White, I. N. H. *Anal. Biochem.* **1988**, *172*, 304.
(19) Auld, D. S.; Veith, H.; Cali, J. J. *Methods Mol. Biol.* **2013**, *987*, 1.
(20) Zhu, B.; Zhang, X.; Jia, H.; Li, Y.; Liu, H.; Tan, W. *Org. Biomol. Chem.* **2010**, *8*, 1650.
(21) Huang, C. S.; Jia, T.; Tang, M. F.; Yin, Q.; Zhu, W. P.; Zhang, C.; Yang, Y.; Jia, N. Q.; Xu, Y. F.; Qian, X. H. *J. Am. Chem. Soc.* **2014**, *136*, 14237.
(22) Xu, Z.; Baek, K. H.; Kim, H. N.; Cui, J.; Qian, X.; Spring, D. R.; Shin, I.; Yoon, J. *J. Am. Chem. Soc.* **2010**, *132*, 601.
(23) Xu, Z.; Singh, N. J.; Lim, J.; Pan, J.; Kim, H. N.; Park, S.; Kim, K. S.; Yoon, J. *J. Am. Chem. Soc.* **2009**, *131*, 15528.
(24) Liu, Z. M.; Feng, L.; Hou, J.; Lv, X.; Ning, J.; Ge, G. B.; Wang, K. W.; Cui, J. N.; Yang, L. *Sens. Actuators, B* **2014**, *205*, 151.
(25) Zeng, X.; Zhang, X.; Zhu, B.; Jia, H.; Li, Y.; Xue, J. *Analyst* **2011**, *136*, 4008.
(26) Zhang, J. F.; Lim, C. S.; Bhuniya, S.; Cho, B. R.; Kim, J. S. *Org. Lett.* **2011**, *13*, 1190.
(27) Liu, T. Y.; Zhang, X. F.; Qiao, Q. L.; Zou, C. Y.; Feng, L.; Cui, J. N.; Xu, Z. C. *Dyes Pigm.* **2013**, *99*, 537.
(28) Zhou, L. Y.; Zhang, X. B.; Wang, Q. Q.; Lv, Y. F.; Mao, G. J.; Luo, A. L.; Wu, Y. X.; Wu, Y.; Zhang, J.; Tan, W. H. *J. Am. Chem. Soc.* **2014**, *136*, 9838.
(29) Yu, H.; Xiao, Y.; Jin, L. *J. Am. Chem. Soc.* **2012**, *134*, 17486.
(30) Zhu, B. C.; Guo, B. P.; Zhao, Y. Z.; Zhang, B.; Du, B. *Biosens. Bioelectron.* **2014**, *55*, 72.
(31) Zhu, B.; Gao, C.; Zhao, Y.; Liu, C.; Li, Y.; Wei, Q.; Ma, Z.; Du, B.; Zhang, X. *Chem. Commun. (Cambridge, U. K.)* **2011**, *47*, 8656.
(32) Loving, G.; Imperiali, B. *J. Am. Chem. Soc.* **2008**, *130*, 13630.
(33) Lee, M. H.; Han, J. H.; Lee, J. H.; Choi, H. G.; Kang, C.; Kim, J. S. *J. Am. Chem. Soc.* **2012**, *134*, 17314.
(34) Srikun, D.; Miller, E. W.; Domaille, D. W.; Chang, C. J. *J. Am. Chem. Soc.* **2008**, *130*, 4596.
(35) Hukkanen, J.; Pelkonen, O.; Hakkola, J.; Raunio, H. *Crit. Rev. Toxicol.* **2002**, *32*, 391.
(36) Bernauer, U.; Heinrich-Hirsch, B.; Tonnies, M.; Peter-Matthias, W.; Gundert-Remy, U. *Toxicol. Lett.* **2006**, *164*, 278.
(37) Racha, J. K.; Rettie, A. E.; Kunze, K. L. *Biochemistry* **1998**, *37*, 7407.
(38) Ge, G. B.; Ning, J.; Hu, L. H.; Dai, Z. R.; Hou, J.; Cao, Y. F.; Yu, Z. W.; Ai, C. Z.; Gu, J. K.; Ma, X. C.; Yang, L. *Chem. Commun. (Cambridge, U. K.)* **2013**, *49*, 9779.
(39) Zanger, U. M.; Schwab, M. *Pharmacol. Ther.* **2013**, *138*, 103.
(40) Ou-Yang, D. S.; Huang, S. L.; Wang, W.; Xie, H. G.; Xu, Z. H.; Shu, Y.; Zhou, H. H. *Br. J. Clin. Pharmacol.* **2000**, *49*, 145.
(41) Liu, X. D.; Hu, L. H.; Ge, G. B.; Yang, B.; Ning, J.; Sun, S. X.; Yang, L.; Pors, K.; Gu, J. K. *Proteomics* **2014**, *14*, 1943.
(42) Tsien, R. Y.; Pozzan, T.; Rink, T. J. *J. Cell Biol.* **1982**, *94*, 325.
(43) Hirayama, T.; Van de Bittner, G. C.; Gray, L. W.; Lutsenko, S.; Chang, C. J. *Proc. Natl. Acad. Sci. U. S. A.* **2012**, *109*, 2228.
(44) Zhang, Z. Y.; Pelletier, R. D.; Wong, Y. N.; Sugawara, M.; Zhao, N. D.; Littlefield, B. A. *Biochem. Biophys. Res. Commun.* **2006**, *341*, 399.
(45) Walsh, A. A.; Szklarz, G. D.; Scott, E. E. *J. Biol. Chem.* **2013**, *288*, 12932.
(46) Bjornsson, T. D.; Callaghan, J. T.; Einolf, H. J.; Fischer, V.; Gan, L.; Grimm, S.; Kao, J.; King, S. P.; Miwa, G.; Ni, L.; Kumar, G.; McLeod, J.; Obach, R. S.; Roberts, S.; Roe, A.; Shah, A.; Snikeris, F.; Sullivan, J. T.; Tweedie, D.; Vega, J. M.; Walsh, J.; Wrighton, S. A.; Pharmaceutical, R.; Manufacturers of America Drug Metabolism/Clinical Pharmacology Technical Working, G.; Evaluation, F. D. A. C. f. D.; Research. *Drug Metab. Dispos.* **2003**, *31*, 815.
(47) Zhang, W. J.; Kilicarslan, T.; Tyndale, R. F.; Sellers, E. M. *Drug Metab. Dispos.* **2001**, *29*, 897.
(48) Yuan, R.; Madani, S.; Wei, X. X.; Reynolds, K.; Huang, S. M. *Drug Metab. Dispos.* **2002**, *30*, 1311.
(49) Rendic, S.; DiCarlo, F. J. *Drug Metab. Rev.* **1997**, *29*, 413.
(50) Kunze, K. L.; Trager, W. F. *Chem. Res. Toxicol.* **1993**, *6*, 649.
(51) Yueh, M. F.; Kawahara, M.; Raucy, J. *Toxicol. In Vitro* **2005**, *19*, 275.
(52) Takahashi, N.; Miranda, C. L.; Henderson, M. C.; Buhler, D. R.; Williams, D. E.; Bailey, G. S. *Comp. Biochem. Physiol., Part C: Pharmacol., Toxicol. Endocrinol.* **1995**, *110*, 273.
(53) Ai, C. Z.; Li, Y.; Wang, Y. H.; Li, W.; Dong, P. P.; Ge, G. B.; Yang, L. *J. Comput. Chem.* **2010**, *31*, 1822.

DOI: 10.1021/jacs.5b09854
J. Am. Chem. Soc. 2015, 137, 14488−14495